Electrically conductive membranes for in situ fouling detection in membrane distillation using impedance spectroscopy

Farah Ejaz Ahmed[1], Nidal Hilal[2] and Raed Hashaikeh[1]*

[1]Department of Chemical Engineering, Khalifa University of Science and Technology Masdar Institute, P.O. Box 54224, Abu Dhabi, United Arab Emirates

[2]Centre for Water Advanced Technologies and Environmental Research (CWATER), College of Engineering, Swansea University, Swansea SA2 8PP, UK

*Corresponding author

Email: rhashaikeh@masdar.ac.ae

Phone: +971-28109152

February 2018

Abstract

Online monitoring of fouling in desalination processes enables early and appropriate action for fouling control. This study demonstrates the use of Electrochemical Impedance Spectroscopy (EIS) to electrically conductive membranes for online monitoring of fouling by eliminating the need for external electrodes and/or canary cells. Electrically conductive membranes are prepared by incorporation of silica in carbon nanostructures and subsequent fluorination to yield hydrophobic membranes. These membranes are applied to direct contact membrane distillation with 99.9% salt rejection and a flux of 4.3 LMH. EIS is used for online monitoring of inorganic fouling on the membrane surface during the MD process. Impedance spectra taken over a duration of 15 hours indicated that impedance in the low frequency (<100 Hz) region gradually decreased with fouling early on, and increased towards the end. Impedance-based monitoring is more sensitive to changes in the system than monitoring of flux and permeate conductivity. It shows the capability of EIS as a sensitive online monitoring tool for fouling in MD.

Keywords: membrane distillation, impedance spectroscopy, fouling, online monitoring, desalination

1. Introduction

Water scarcity around the world combined with government regulations on water quality have driven research in desalination, in which membrane technology has played a significant role. At present, reverse osmosis accounts for 60% of the world's desalination capacity [1], but the high energy costs associated with the process have caused research in other desalination technologies such as membrane distillation (MD) to gain momentum over the last decade. MD is a separation process in which a temperature difference is applied across a porous hydrophobic membrane, and the resulting vapor pressure difference allows clean water vapor to pass through. Although traditionally used for desalination, MD can also be applied to separation of pharmaceutical compounds, juices, dairy compounds and treatment of produced water [2]. Direct contact membrane distillation (DCMD) is the simplest configuration of MD in which the two sides of the membrane are directly in contact with the hot feed and cold permeate.

As with other membrane-based processes, fouling - or the unwanted deposition of feed substances on the membrane, remains a cause for concern in MD. Fouling leads to lower productivity and reduced permeate quality. Currently, observation of the transmembrane flux and salt rejection provide an indication of the extent of fouling; however by the time a significant change is measured, the effects of fouling are already significant. A fast and sensitive tool for the detection of fouling is crucial for fouling control measures to be taken in a timely manner.

Electrochemical impedance spectroscopy (EIS) is a powerful characterization tool commonly used to study electrochemical devices, coatings, etc. Interest in the use of EIS for monitoring membrane processes has augmented recently. Changes due to the foulant layer may be observed by measuring impedance. EIS has recently been used to monitor inorganic as well as organic

fouling in polymeric membranes in reverse osmosis [3, 4], microfiltration, ultrafiltration [5] and nanofiltration [6]. EIS has already been used for online monitoring of fouling in an RO plant field trial using a canary cell [4]. They found that changes in impedance could be used as a method for early detection of fouling as compared to the conventional methods of observing changes in flux and salt rejection. These studies require the use of a canary cell fitted with electrodes into which a bypass of the feed stream is sent and operating conditions are made to resemble that of the membrane module . Electrically conductive membranes [7, 8] and spacers [9] can be used for fouling detection and control in separation processes, eliminating the need for external electrodes and/or the use of canary cells [4]. Recently, MD was combined with an electrochemical system for wetting detection by: (i) monitoring the current [10] and (ii) by monitoring impedance [11].

Carbon nanotube membranes have gained attention over the last decade. In addition to DCMD [12, 13], CNT membranes have also been used in microfiltration, ultrafiltration [14], nanofiltration [15, 16] as well as reverse osmosis [17]. Carbon nanostructures (CNS), made of entangled covalently bonded multiwalled CNTs, have previously previously been used as membranes for microfiltration and nanofiltration [8, 18]. CNS are characterized by improved processability, high electrical conductivity and large surface area [19].

In this work, electrically conductive membranes have been prepared by incorporation of silica gel and an additive [either polyvinyl alcohol (PVA) or networked cellulose (NC) [20]] in carbon nanostructures, calcination and subsequent fluorination to yield conductive hydrophobic membranes. The effect of the type of additive used on the membranes was studied in terms of morphology, hydrophobicity and pore size. The conductive membranes were then applied to DCMD of saltwater with colloidal silica used as an inorganic foulant and online EIS was carried

out to detect changes on the membrane over time. To the best of our knowledge, this is the first study in which EIS is applied to detect fouling during MD using an electrically conductive membrane. The canary cell system described earlier is more of a sampling system, while this study demonstrates in situ monitoring of actual membrane fouling in MD.

2. Materials and Methods

Carbon Nanostructures (average length ~300 nm) were obtained from Applied NanoStructured Solutions LLC (ANS). Sodium chloride (NaCl), polyvinyl alcohol (Mowiol 18-88, M_w: 130 kDa), colloidal silica (LUDOX HS-30), Tetraethyl Orthosilicate (TEOS), hydrochloric acid (HCl) and 2H, 2H-Perfluorodecyltrichlorosilane (FDTS, 97%) were all purchased from Sigma Aldrich. Ethanol absolute was obtained from VWR International.

2.1 Fabrication

CNS flakes (100 mg) were dispersed in a 1:1 (v/v) ethanol/DI water mixture using a probe sonicator (Hielscher, UP400S) at 50% amplitude and 0.5 cycle for 1 hour before the addition of silica. Silica gel was used in order to facilitate fluorination to tune membrane hydrophobicity. Silica sol-gel solution was obtained from an acid-catalzed TEOS system, as described by Buckley and Greenblatt [21]. In short, 30 mL of TEOS was poured into a round flask and 31 mL of ethanol was stirred in as the solvent. A few drops of HCl was added to 38 mL of DI water and stirred into the solution for over an hour. 10 mL of the silica sol-gel solution was then added to the CNS dispersion. PVA or NC were used as an additive and later removed during the calcination process in order to control the pore size of the CNS membranes. Either 5 mL of 5 wt. % PVA solution in DI water or 0.5 g of networked cellulose (NC) were added to the CNS dispersion and further sonicated for 1 hour, yielding an ink like homogeneous suspension. The CNS-PVA-silica or CNS-NC-silica suspension was vacuum filtered through a 6.5 cm diameter

filter and the filter paper was peeled. The wet membrane was freeze dried using wizard 2.0 Virtis freeze drier. Calcination at 350 °C was carried out to remove PVA. A schematic of how freeze drying of a polymer solution can be used to introduce porosity is shown in **Figure 1**.

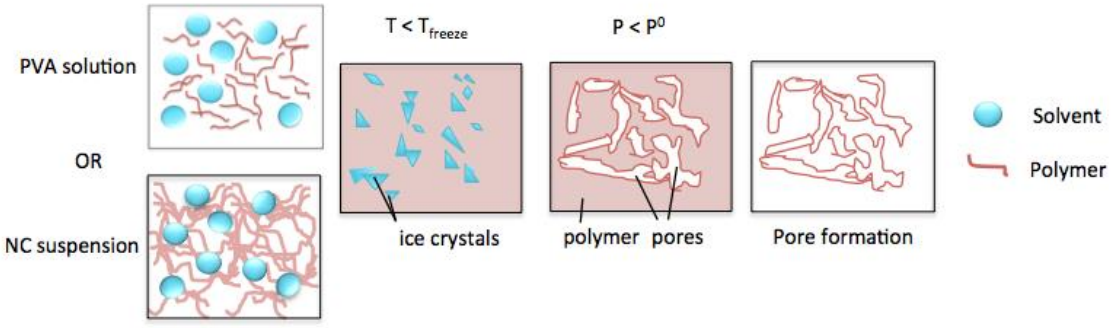

Figure 1: Schematic showing pore formation mechanism using freeze drying; T_{freeze} and P^0 are the freezing point and equilibrium vapor pressure of the solvent respectively

Drying and calcining in the sol-gel are critical to the sol gel process, where drying is done to remove fluids and calcination is carried out to eliminate residual organic groups, densify the silica gel [22] and in this case, also remove the PVA or NC additive. For fluorination of the membranes, a clear solution of FDTS in ethanol (0.25 w/v %) was prepared. The membranes were immersed in FDTS solution and air dried before being heat treated in an oven at 100 °C for 2 hours. The fluorination procedure was carried out three times to ensure fluorination and the contact angle was measured before and after.

Table 1: Content of CNS:silica in final membrane and type of additive used

Sample	CNS	Silica	Additive
C-Si-PVA-F	10 wt. %	90 wt. %	PVA
C-Si-NC-F	10 wt. %	90 wt. %	NC

2.2 Characterization

2.2.1 Morphology

The effect of additives was investigated in terms of morphology of the membrane surface, which was examined using high-resolution scanning electron microscopy (FEI Nova NanoSEM, Netherlands) under high vacuum.

2.2.2 Contact angle

Contact angle tests were carried out for the membranes before and after fluorination at room temperature using an EasyDrop Standard drop shape analysis (KRUSS, Germany). A 4 μL droplet of DI water was produced on the membrane and the digital image was used to determine contact angle. The contact angle was measured three times for each sample, using all three methods (sessile drop, tangent line and circle fitting), and the average was recorded.

2.2.3 Pore size and porosity

Mean pore size and bubble point of the membranes was obtained with PMI Capillary Flow Porometer (PMI, Ithaca, NY-USA). Membrane samples (2.5 cm diameter) were first wetted with Galwick (surface tension: 15.9 dynes/cm) and then the liquid was displaced from pores using a pressurized gas. The instru- ment determines the largest pore and the mean pore size from the gas pressure needed to remove liquid from pores.

Membrane porosity was measured by completely filling the pores of a membrane sample of known weight and dimensions with a highly wetting liquid of surface tension of 20.1 dynes/cm (Silwick®, provided by PMI, Ithaca, NY, USA). Pore volume was determined from the weight difference between dry and wet samples and density of the wetting liquid and porosity was calculated as the ratio of pore volume to sample volume.

2.2.4 Liquid entry pressure (LEP)

Liquid entry pressure of a membrane measures the minimum value of the hydrostatic pressure required for a given liquid, in this case water, to penetrate the largest membrane pores. It is given by:

$$\Delta P_{entry} = \frac{-2B\gamma_L \cos\theta}{d_{max}} \quad (1)$$

where B is a geometric shape factor, γ_L is the surface tension of the solution, θ is the contact angle between the liquid and the membrane surface and d_{max} is the largest pore radius.

LEP was measured using Convergence Liquid Entry Pressure tester. LEP is measured by increasing the pressure in increments to the point where the liquid permeates through the membrane, indicated by a pressure drop. The system is first deaerated for 40 seconds, and the pressure is then increased from 0.5 – 5.9 bars with a step size of 0.1 bar and a waiting time of 20 seconds per step. Each sample was run twice.

2.3 MD-EIS

MD-EIS was carried out in a custom built system with a flat membrane sample of 3.5 cm x 5.5 cm as working electrode. A stainless steel counter electrode was fitted on the feed side. A solution of 2000 ppm NaCl in DI water was used as feed, colloidal silica added to a final concentration of 200 ppm as inorganic foulant. Pure DI water was used as the permeate. The flow rate on both permeate and feed sides was kept at 0.8 L/min. The feed temperature was maintained at 70 °C, while the permeate was kept at 30 °C. The fouling agent was added after 1 hour of membrane distillation with saltwater on one side and DI water on the other. Testing was carried out for 15 hours. Permeate TDS was measured using an Accumet XL50 (Fisher

Scientific) conductivity meter, and the flux was measured using a balance. Salt rejection was calculated from the salinity of the feed and permeate using the following equation:

$$\eta = \frac{C_{feed}-C_{filtrate}}{C_{feed}} \text{ x } 100 \quad (2)$$

Impedance measurements were carried out using a two electrode system during DCMD operation on Autolab PGSTAT 302N. Usually a 4 terminal method is used in fouling monitoring to account for the effects of voltage electrode-solution interfaces, but in this case since the membrane itself is conductive and acts as an electrode, a four electrode system is not needed. An alternating voltage of 100 mV was applied at 50 frequencies over a range of 10^{-2} to 10^{5} Hz in a logarithmic distribution, and the current developed was used to calculate the impedance. The potentiostat has a current accuracy of ±0.2%. Impedance spectra were obtained regularly during the 15 hour MD process (at t = 0h, 2h, 3h, 4h, 5h, 6h, 7h, 8h, 9h, 10h, 11h, 12h, 15h) to monitor changes in fouling. Each measurement took about 12 minutes.

3. Theory and equivalent circuit model

Potentiostatic EIS is a non-invasive characterization technique in which a small amplitude sinusoidal potential $v = v_0 \sin(\omega t)$ is applied to a system at a given frequency and the current response that develops with the same frequency but different amplitude i_0 and phase is measured.

Impedance spectroscopy is carried out by injecting an AC voltage $v = v_0 \sin(\omega t)$ of known frequency ω across an electrochemical system, in this case a system made of two electrodes (membrane as the electrode and a stainless steel counterelectrode), with the feed solution between them. The current response through the system is digitally computed, and can be expressed as:

$i = i_0\,(\omega t + sin\,\theta)$ (3),

where i_0 is the current amplitude and θ is the phase difference.

The measured impedance is expressed as

$$Z(\omega) = \frac{v_0}{i_0}(\cos\theta + j\sin\theta) \quad (4)$$

where j is the imaginary constant defined by $j^2 = -1$. The parameters above yield impedance magnitude $|Z| = \frac{v_0}{i_0}$ and phase θ. The impedance is measured over a range of frequencies.

The admittance, which is the reciprocal of the impedance, is defined as:

$$Y(\omega) \equiv \frac{1}{Z(\omega)} \equiv G(\omega) + j\omega C(w) \quad (5)$$

where the conductance G is the ability of the system to conduct electric charge, and the capacitance C is the ability of the system to store electric charge [23]. Each layer can be represented by a conductive and capacitive component such that overall G and C have a frequency dependence. These parameters are often expressed in terms of area of the measurement,

$$y(\omega) \equiv \frac{Y(\omega)}{A} \equiv \frac{G(\omega)}{A} + j\omega\frac{C(\omega)}{A} \equiv g(\omega) + j\omega c(w) \quad (6)$$

The impedance, conductance and capacitance spectra are then observed over a range of frequencies to study changes in the system. Nova 1.10 was used to fit an equivalent circuit model to the data. The goodness of the fit is indicated by the χ^2 value. The software used a least-squares-error method under the following preset convergence conditions:

- maximum number of iterations: 500;
- maximum number of iterations without improvement: 100;

- maximum change in χ^2 parameter 0.001.

4. Results and Discussion

4.1 Morphology

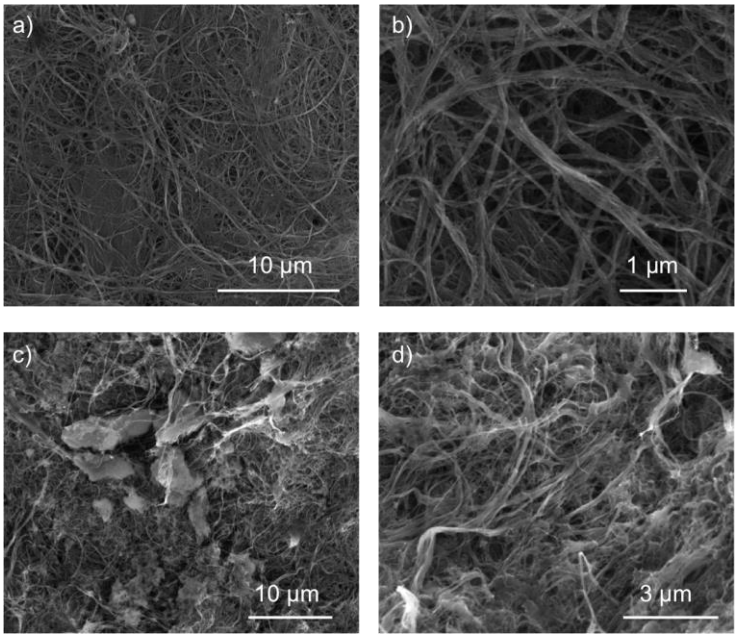

Figure 2: SEM images of the surfaces of the a) and b) C-Si-PVA-F, and c) and d) C-Si-NC-F membranes at different magnification.

Figure 2 shows the SEM images of the surface of the two membranes fabricated using different additives. Even though the additives are removed during the calcination step, each of them have a distinct effect on the morphology of the final membrane. While the membrane made with PVA as additive appears flat with a surface composed of entangled CNTs (**Figure 2a and b**), the membrane made with NC appears to have a fluffy or foamy morphology (Figure 2c and d), and still appears to hold cellulose residue. Pure PVA generally decomposes below 350 °C, as shown in TGA studies in literature [24, 25], whereas in the case of NC, although maximum weight loss occurs at ~324 °C [20], it does not completely degrade at the specified calcination temperature of 350 °C.

4.2 Contact angle

Figure 3 shows a water droplet on the two membranes after fluorination. The hydrophilic nature of the membranes before fluorination can be observed in the videos in the supplementary section. Fluorination of the silica allows control of wettability and yields hydrophobic membranes, as shown in **Figure 3a**.

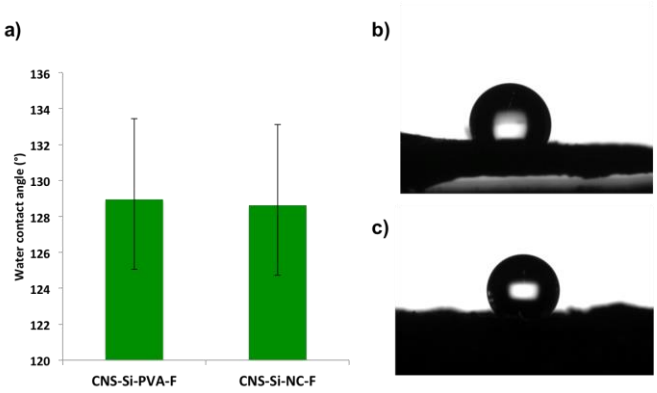

Figure 3: contact angle of cns-silica membranes and images of water droplets on the surface of b) CNS-silica-PVA-F and b) CNS-silica-NC-F membranes

4.3 Pore size and porosity

Table 2 lists the bubble point, mean pore size and porosity of the two membranes. The pore size of the membranes prepared with PVA was significantly smaller and closer to that of CNS reported in previous studies [8]. However, when NC was used as an additive and then calcined, the resulting pore size is significantly increased (**Table 2**), although the porosity of both membranes is still low.

Table 2: Bubble point, mean pore size and porosity of cns-silica membranes

	Bubble point (µm)	**Mean pore size (µm)**	**Porosity (%)**
C-Si-PVA-F	0.19	0.0889 ± 0.01 µm	47 ± 4
C-Si-NC-F	1.1	0.861± 0.15 µm	52 ± 8

4.4 Liquid entry pressure

Figure 4 shows the LEP of the two membranes. Despite similar contact angles, C-Si-PVA-F has a slightly higher LEP than C-Si-NC-F, due to the smaller pores. As shown above, LEP is inversely related to the maximum pore size.

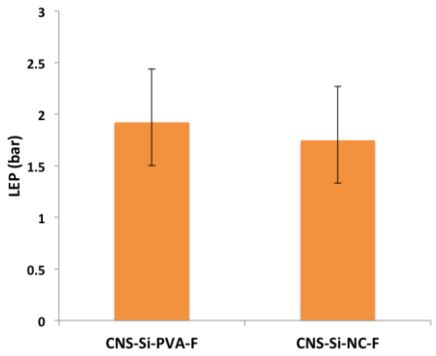

Figure 4: LEP of CNS-silica membranes after fluorination

4.5 Membrane performance for MD

MD was carried out using CNS-silica-PVA-F membrane for 15 hours. **Figure 5** shows the flux and salt rejection of the membrane during DCMD. Salt rejection remained above 99.8%, with a decline of <1% during the 15 hour period. This salt rejection is possible due to the non-wetting characteristic of the membrane, reflected by its high LEP and water contact angle. However, the flux of the membrane was low (4.3 $L^{m-2}h^{-1}$). This could be attributed to mass transfer resistance in the form of large membrane thickness (1.3 mm), as well as and the relatively low porosity of the membrane (47%).

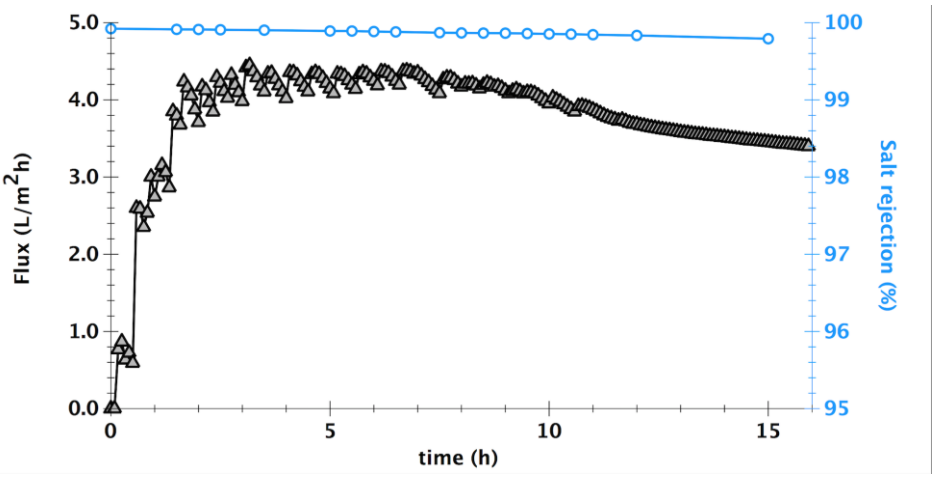

Figure 5: Flux and salt rejection through CNS-silica-PVA membrane during DCMD of saltwater (2000 ppm) and colloidal silica (200 ppm)

4.6. MD-EIS

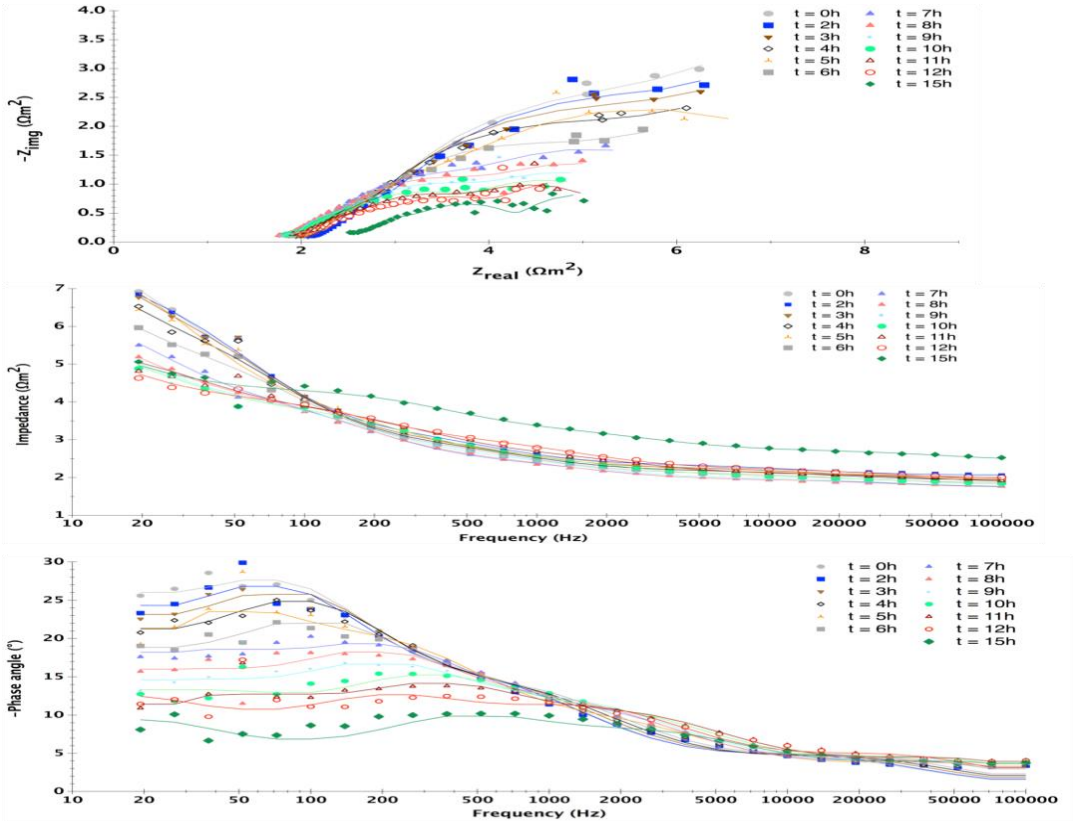

Figure 6: a) Nyquist plot, b) Impedance modulus and c) Phase angle obtained from EIS during DCMD of saltwater (2000 ppm) with inorganic foulant (200 ppm) using C-Si-PVA-F membrane. The curves show fitting of the equivalent circuit model to the data points

Figure 6 shows impedance spectra for the MD process at different times. In general, impedance decreases with frequency, however only the low-frequency region (<100 Hz) is of interest when studying membrane fouling as indicated in previous impedance studies for RO fouling [23, 26]. This is because low frequencies relate to the diffusion polarization regime which corresponds to the electrode-solution interface, or the region at the membrane surface, where fouling occurs. As shown in **Figure 6b**, there is no significant change in impedance in the first 3 hours (<1 %), after which impedance gradually decreases as fouling progresses with the impedance at 11h being 30% less than the starting impedance. At a later stage (t = 15h), the impedance slightly increases. Gradual reduction in impedance with the progression of fouling is not detectable through observation of permeate flux and salt rejection (**Figure 5**).. Another representation of the impedance data is on the complex plane, shown in **Figure 6a**. The diameter of the semicircle, which indicates the real or resistive part of the impedance, continues to decrease with time.

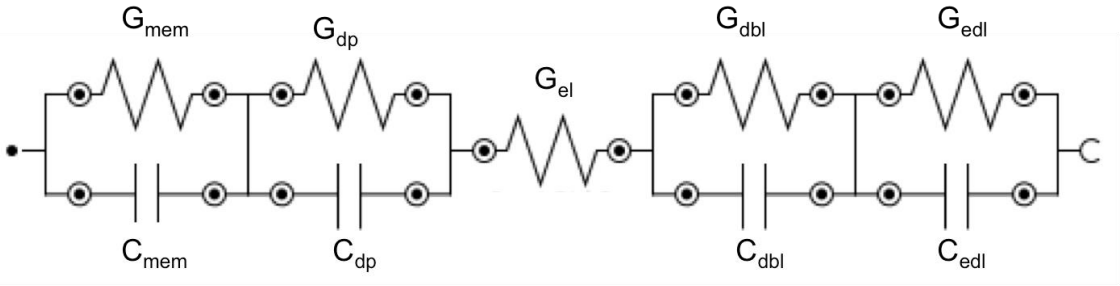

Figure 7: Equivalent circuit model used to fit data

Data was fitted to an equivalent circuit model shown in **Figure 7**. At the counter electrode, two layers (each with a capacitive and conductive component) reflect the inner electrical double layer (G_{edl}, C_{edl}), and an outer more diffuse layer ($G_{dbl,}$ C_{edl}) of more loosely bond ions [27]. G_{el} refers to the resistance of the electrolyte solution. On the other hand, the porosity of the membrane contributes to a parallel conductance and capacitance indicated by G_{mem} and C_{mem} respectively. G_{dp} and C_{dp} correspond to the diffusion polarization regime at the membrane-solution interface.

Diffusion polarizaion refers to the accumulation and depletion of ions near the surface when a bias is applied, and its effect is predominant at low frequencies when ions have enough time to respond to the change in bias of the membrane. While the conductance and capacitance for each layer do not vary with frequency, the overall conductance and capacitance are functions of frequency. Capacitance spectra for the membrane with progression of fouling during MD is shown in **Figure 8.**

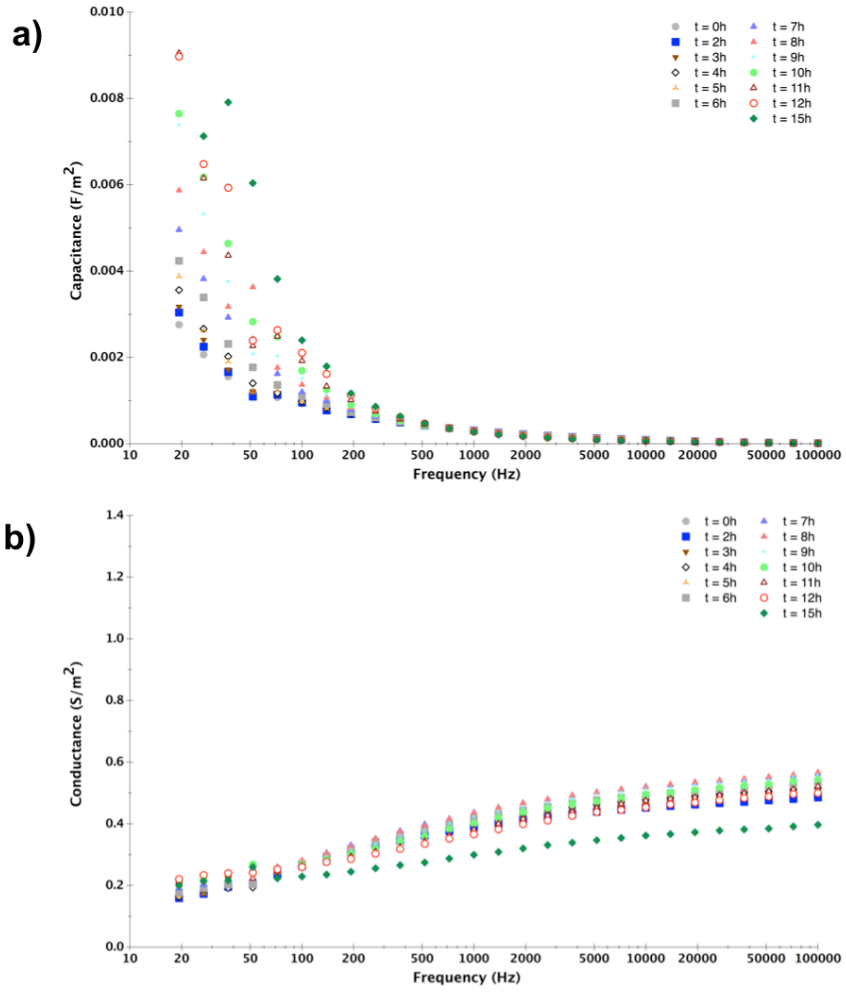

Figure 8: Capacitance and conductance spectra obtained from EIS for CNS-Si-PVA-F membrane during DCMD

Capacitance starts to increase early on and continues to increase as the foulant layer accumulates on the membrane surface, increasing the dielectric space between the conductive membrane surface and oppositely charged ions in the electrolyte, as shown in the schematic in **Figure 9**. Hence, EIS has been shown to indicate early on how foulant starts to accumulate on the surface of a conductive MD membrane. This increase in capacitance is also reflected by the gradual decrease in phase angle (**Figure 6c**). It is interesting to note that the decline observed in salt rejection over the period of 15 hours was too small (<1%) to give any insight into the progress of fouling, while a noticeable flux decline (15%) was observed after 12 hours when the foulant had likely blocked pores. This is also reflected in the conductance data that shows an increase at 15 hours due to a denser fouling layer.

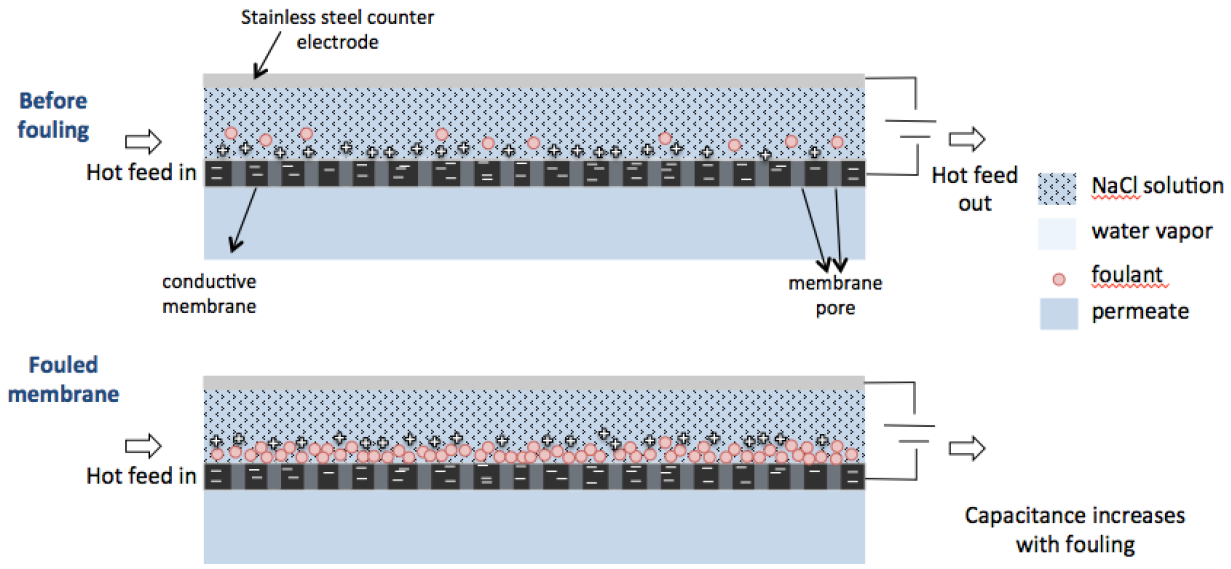

Figure 9: Schematic shows fouling mechanism that leads to observed increase in capacitance

5. Conclusion

Wetting in MD is a major concern that prevents commercialization. Membrane fouling is a main cause for the wetting phenomena. Successful detection of fouling in situ can be the solution for

this operation problem. EIS is a potential technique to detect in situ fouling without any interference with the MD process operation. In order to use the EIS technique directly on membranes, the membranes have to be electrically conductive. Electrically conductive membranes were prepared from CNS-silica using two different additives. The pore size and wettability could be controlled by choosing the appropriate additive and via fluorination of the silica. These conductive hydrophobic membranes were applied for DCMD of saltwater using an inorganic foulant and simultaneous EIS was carried out in place. It was found that impedance data could be used to observe the effect of the foulant earlier than changes in flux decline and salt rejection. While the impedance did not significantly change in the first 2 hours of operation, it then began to decrease possibly due to the combined effects of fouling and resulting penetration of water. In later stages when the foulant layer was formed on the membrane, the impedance decreases. Although the flux of these membranes is still quite low, it provides a valuable insight into the use of electrically conductive membranes, potential for them to further modified and used directly as electrodes in the MD process for online monitoring.

6. Acknowledgements

The authors would like to thank Lockheed Martin for providing CNS and funding this study.

7. References

[1] M. Baawain, B.S. Choudri, M. Ahmed, A. Purnama, Recent Progress in Desalination, Environmental and Marine Outfall Systems, Springer International Publishing, 2015.

[2] E. Drioli, A. Ali, F. Macedonio, Membrane distillation: Recent developments and perspectives, Desalination, 356 (2015) 56-84.

[3] J.M. Kavanagh, S. Hussain, T.C. Chilcott, H.G.L. Coster, Fouling of reverse osmosis membranes using electrical impedance spectroscopy: Measurements and simulations, Desalination, 236 (2009) 187-193.

[4] J.S. Ho, L.N. Sim, R.D. Webster, B. Viswanath, H.G.L. Coster, A.G. Fane, Monitoring fouling behavior of reverse osmosis membranes using electrical impedance spectroscopy: A field trial study, Desalination, 407 (2017) 75-84.

[5] L. Gaedt, T.C. Chilcott, M. Chan, T. Nantawisarakul, A.G. Fane, H.G.L. Coster, Electrical impedance spectroscopy characterisation of conducting membranes, Journal of Membrane Science, 195 (2002) 169-180.

[6] Y. Xu, M. Wang, Z. Ma, C. Gao, Electrochemical impedance spectroscopy analysis of sulfonated polyethersulfone nanofiltration membrane, Desalination, 271 (2011) 29-33.

[7] R. Hashaikeh, B.S. Lalia, V. Kochkodan, N. Hilal, A novel in situ membrane cleaning method using periodic electrolysis, Journal of Membrane Science, 471 (2014) 149-154.

[8] B.S. Lalia, F.E. Ahmed, T. Shah, N. Hilal, R. Hashaikeh, Electrically conductive membranes based on carbon nanostructures for self-cleaning of biofouling, Desalination, 360 (2015) 8-12.

[9] H.S. Abid, B.S. Lalia, P. Bertoncello, R. Hashaikeh, B. Clifford, D.T. Gethin, N. Hilal, Electrically conductive spacers for self-cleaning membrane surfaces via periodic electrolysis, Desalination, 416 (2017) 16-23.

[10] F.E. Ahmed, B.S. Lalia, R. Hashaikeh, Membrane-based detection of wetting phenomenon in direct contact membrane distillation, Journal of Membrane Science, 535 (2017) 89-93.

[11] Y. Chen, Z. Wang, G.K. Jennings, S. Lin, Probing Pore Wetting in Membrane Distillation Using Impedance: Early Detection and Mechanism of Surfactant-Induced Wetting, Environmental Science & Technology Letters, (2017).

[12] L.F. Dumée, K. Sears, J. Schütz, N. Finn, C. Huynh, S. Hawkins, M. Duke, S. Gray, Characterization and evaluation of carbon nanotube Bucky-Paper membranes for direct contact membrane distillation, Journal of Membrane Science, 351 (2010) 36-43.

[13] L. Dumée, V. Germain, K. Sears, J. Schütz, N. Finn, M. Duke, S. Cerneaux, D. Cornu, S. Gray, Enhanced durability and hydrophobicity of carbon nanotube bucky paper membranes in membrane distillation, Journal of Membrane Science, 376 (2011) 241-246.

[14] B. Lee, Y. Baek, M. Lee, D.H. Jeong, H.H. Lee, J. Yoon, Y.H. Kim, A carbon nanotube wall membrane for water treatment, 6 (2015) 7109.

[15] F.E. Ahmed, B.S. Lalia, N. Hilal, R. Hashaikeh, Electrically conducting nanofiltration membranes based on networked cellulose and carbon nanostructures, Desalination, 406 (2017) 60-66.

[16] M.-B. Wu, Y. Lv, H.-C. Yang, L.-F. Liu, X. Zhang, Z.-K. Xu, Thin film composite membranes combining carbon nanotube intermediate layer and microfiltration support for high nanofiltration performances, Journal of Membrane Science, 515 (2016) 238-244.

[17] Q. Tu, Q. Yang, H. Wang, S. Li, Rotating carbon nanotube membrane filter for water desalination, 6 (2016) 26183.

[18] F.E. Ahmed, B.S. Lalia, N. Hilal, R. Hashaikeh, Electrically conducting nanofiltration membranes based on networked cellulose and carbon nanostructures, Desalination, 406 (2017) 60-66.

[19] T.K. Shah, H.C. Malecki, R.R. Basantkumar, H. Liu, C.A. Fleischer, J.J. Sedlak, J.M. Patel, W.P. Burgess, J.M. Goldfinger, Carbon nanostructures and methods of making the same, in, Google Patents, 2013.

[20] R. Hashaikeh, H. Abushammala, Acid mediated networked cellulose: preparation and characterization, Carbohydrate polymers, 83 (2011) 1088-1094.

[21] A.M. Buckley, M. Greenblatt, The Sol-Gel Preparation of Silica Gels, Journal of Chemical Education, 71 (1994) 599.

[22] W.L. Huang, K.M. Liang, S.R. Gu, Calcining silica gels at different drying stages, Materials Letters, 46 (2000) 136-141.

[23] A. Antony, T. Chilcott, H. Coster, G. Leslie, In situ structural and functional characterization of reverse osmosis membranes using electrical impedance spectroscopy, Journal of Membrane Science, 425–426 (2013) 89-97.

[24] J.W. Gilman, D.L. VanderHart, T. Kashiwagi, Thermal Decomposition Chemistry of Poly(vinyl alcohol), in: Fire and Polymers II, American Chemical Society, 1995, pp. 161-185.

[25] B. Gupta, R. Agarwal, M. Sarwar Alam, Preparation and characterization of polyvinyl alcohol- polyethylene oxide- carboxymethyl cellulose blend membranes, Journal of Applied Polymer Science, 127 (2013) 1301-1308.

[26] J. Cen, J. Kavanagh, H. Coster, G. Barton, Fouling of reverse osmosis membranes by cane molasses fermentation wastewater: detection by electrical impedance spectroscopy techniques, Desalination and Water Treatment, 51 (2013) 969-975.

[27] E. Fontananova, W. Zhang, I. Nicotera, C. Simari, W. van Baak, G. Di Profio, E. Curcio, E. Drioli, Probing membrane and interface properties in concentrated electrolyte solutions, Journal of Membrane Science, 459 (2014) 177-189.